Cu and Zn stable isotopes in suspended particulate matter sub-fractions from the Northern Bay of Biscay help identify biogenic and geogenic particle pools

Daniel Ferreira Araujo, Joël Knoery, Nicolas Briant, Emmanuel Ponzevera, Daniel Santos Mulholland, Sandrine Bruzac, Teddy Sireau, Tiphaine Chouvelon, Christophe Brach-Papa

Version of Record: https://www.sciencedirect.com/science/article/pii/S0278434322001443
Manuscript_22e550ad0f623a025277397fe23b2157

Cu and Zn stable isotopes in suspended particulate matter sub-fractions from the Northern Bay of Biscay help identify biogenic and geogenic particle pools

Daniel F. Araújo[a]*, Joël Knoery[a], Nicolas Briant[a], Emmanuel Ponzevera[a], Daniel Santos Mulholland[b] Sandrine Bruzac[a], Teddy Sireau[a], Tiphaine Chouvelon[a-c], Christophe Brach-Papa[d]

a. Ifremer, CCEM Centre Atlantique, Unité Contamination Chimique des Écosystèmes Marins, F-44000 Nantes, France
b. Laboratório de Águas e Efluentes & Laboratório de Análises Ambientais, Universidade Federal do Tocantins, Rua Badejos, Gurupi, TO – Brasil
c. Observatoire Pelagis, UAR 3462 La Rochelle Université-CNRS, 17000 La Rochelle, France
d. Ifremer, Centre Méditerranée, Unité Littoral, Laboratoire Environnement Ressources Provence-Azur-Corse (LERPAC), 83507, La Seyne-sur-Mer Cedex, France

Abstract

Marine suspended particulate matter (SPM) plays a pivotal role in the marine biogeochemical cycling of trace elements. This study investigates metal distributions and copper (Cu) and zinc (Zn) stable isotope ratios in different size fractions of SPM from two sampling stations on the inner continental shelf of northern Bay of Biscay (NE Atlantic), a zone highly influenced by the macrotidal Loire estuary, the outlet of a major European river. The objective of this study is to test stable isotopes as tools to infer the origins of particles and their formation processes, and to infer relevant Cu and Zn biogenic pools involved in marine trophic transfers of these metals. SPM samples were nearly quantitatively mineralized (i.e., without HF) to determine metals and Cu and Zn isotopes in their more labile and reactive phases. Their $\delta^{65}Cu_{SRM\text{-}976}$ values ranged from -0.45 to +0.51‰, with higher Cu concentrations accompanying particle size decreasing. The $\delta^{66}Zn_{JMC\text{-}Lyon}$ values in SPM sub-fractions varied from +0.14 to +0.76‰, and were uncorrelated to both Zn concentrations and particle size. Compared to larger size fractions, increased Al and Fe levels (proxies for terrigenous materials) and enrichments in lighter Cu and Zn isotopes observed in the smaller size SPM sub-fractions suggest that a major proportion of SPM Cu and Zn is associated with geogenic particles. Conversely, the relative enrichment of heavy isotopes in coarser particles is attributable to an increase of Cu and Zn metabolically incorporated into biogenic organic particles (e.g., plankton), and by surface adsorption onto organic detrital particles. The higher δ-values attributed to biogenic particles likely represents the isotope composition of the local marine organic matter available to primary consumers like filter-feeders (oysters). Thus, this study shows that targeting particles of specific size classes allows to identify relative dominances of biogenic and geogenic carrier phases. Identifying these pools and their isotopic composition may help track Cu and Zn transfers through marine food-web metal in future studies.

Keywords: Biscay Bay; Loire estuary; trace metal biogeochemistry; isotope tracer; Cu and Zn stable isotopes; MC-ICP-MS

1. Introduction

In aquatic environments, suspended particulate matter (SPM) plays a pivotal role in controlling reactivity, transport and biological uptake of trace elements (Dang, Schäfer, et al., 2015; Mason, 2013; Petit et al., 2015; Turner & Millward, 2002). It encompasses a wide range of particle sizes, from nanometers to millimeters, and includes a combination of allochthonous and autochthonous compounds of lithogenic, hydrogenic, biogenic and anthropogenic origins (Lam et al., 2018; Schulz & Zabel, 2006; Turner & Millward, 2002). It accounts for various organic compounds, including biofilms coated on clay mineral surfaces that can modify the surface texture and act as a cementing agent for sediment particles (Coutaud et al., 2014; Turner & Millward, 2002).

Trace metals can be associated with SPM as lattice structural components, or interact physico-chemically with them via adsorption, complexation, occlusion and (co)-precipitation processes (Brown & Calas, 2011; Dekov et al., 2014; Köbberich & Vance, 2018; Sparks, 2005; von der Heyden & Roychoudhury, 2015). Geochemical and biological processes (such as weathering, primary activity and hydrology) modulate interactions and distributions of trace metals in the different physicochemical SPM sub-fractions (Bianchi, 2007; de Souza Machado et al., 2016; Sparks, 2005; Tonhá et al., 2020). Therefore, their analysis in target particle classes can provide information about underlying biogeochemical processes controlling the behavior of these elements in aquatic systems, including continental shelves.

In recent years, the determination of stable copper (^{65}Cu, ^{63}Cu) and zinc (^{64}Zn, ^{66}Zn, ^{67}Zn, ^{68}Zn, ^{70}Zn) isotope abundances in environmental matrices have emerged as a new tool to examine the origins and interactions of these elements with compounds in the aquatic environment, including particles and dissolved ligands (Albarède et al., 2016; Ducher et al., 2016; Moynier et al., 2017). Heavy and light isotopes of these elements exhibit subtle differences in their chemical reactivities related to bond energies. They are unevenly distributed among reactants and products, phases, molecules, or compartments, involved in biogeochemical processes: biological uptake, redox reactions, scavenging and others (Araújo et al., 2022; Fujii et al., 2014; Little et al., 2014; Sherman & Little, 2020; Wiederhold, 2015). This isotope fractionation phenomenon occurs in a variety mechanisms and magnitudes, yielding isotope ratio changes that allow tracking Cu and Zn controlling processes (Aranda et al., 2012; Borrok et al., 2008; Skierszkan et al., 2016; Viers et al., 2018; Weiss et al., 2007).

In aquatic systems, the characterization of Cu and Zn isotope signatures of SPM present in fluvial, lacustrine and estuarine environments has been used to trace the sources and sinks of these elements (Araújo et al., 2017; Babcsányi et al., 2014; El Azzi et al., 2013; Guinoiseau et al., 2018; Liang et al., 2020; Peel et al., 2009; Petit et al., 2013, 2015). However, isotope description of the distribution of these elements in different size classes of aquatic SPM is lacking and hence, deserves major investigations. Since particle size depends only on weathering processes, biological activity and contaminant transport in the watersheds (Chester, 2003; Schulz & Zabel, 2006; Unda-Calvo et al., 2019), describing Cu and Zn isotope compositions in the different size classes of SPM sub-fractions can provide additional information about sources and processes that is not accessible when analyzing only bulk SPM. For an example, in the context of Cu-contaminated soils by vineyard activity, analyses of silt and fine clay fractions of the soils showed distinct Cu isotope compositions related to the mineralogical and geochemical phases (Babcsányi et al., 2016; El Azzi et al., 2013). In atmospheric environments, Cu and Zn isotope distribution among particle size fractions of mineral dust presented a "U-shape" pattern, with lighter isotopic compositions in the mid particle size fractions and heavier isotopic compositions in the smaller and larger particles (Schleicher et al., 2020).

To date, however, very little Cu and Zn isotope data exist for particulate material from the marine water column (Little et al., 2018). To fill this gap, this preliminary study examines possible Cu and Zn isotope variability in different particle size classes of the SPM from the northern Bay of Biscay (NE Atlantic), a local influenced by the macrotidal Loire estuary. We targeted the Cu and Zn isotopes in labile, reactive and biologically available fractions of particles, rather than the Cu and Zn atoms from solid lattice structures by using a "pseudo" total extraction (without hydrofluoric acid). With this approach, we intend to link the observed isotope patterns with biogeochemical processes, in order to constrain particle origins (inorganic *vs.* organic, natural *vs.* anthropogenic) and to identify the bioorganic pools (*e.g.*, plankton) that are relevant in transferring Cu and Zn to upper trophic levels. Analyses of other trace and major elements are used to support the discussion.

2. Methods

2.1 SPM sampling and preparation

The Bay of Biscay is an open oceanic basin in the north-eastern Atlantic Ocean, fringed by the Spanish and French coasts (Fig. 1). The continental shelf is up to about 100 miles (160 km) wide off the coast of Brittany but narrows to less than 65 km off the Spanish shore. The

counterclockwise surface currents of the Biscay Bay are influenced by the circulation in the North Atlantic. From mid-autumn to early spring (thus including winter as a whole), intense river flows associated with sustained wind activity maintain this region under the influence of the northward plumes of the Gironde and Loire rivers along the coast, with relatively low salinities between the coast and the 100 m isobath, at around 20–40 km from the coast (Penaud et al., 2020). Freshwater discharges from the main rivers (Loire, Gironde, Vilaine and Adour; cumulative annual mean flow around 4200 m^3/s) in surface layers thus induce steep density gradients driving a poleward circulation (about 10 cm/s) modulated by wind forcing (Lazure et al., 2008; Lazure & Jegou, 1998). The climate on shore is maritime, with mild winters and cool summers (Penaud et al., 2020).

The macrotidal Loire estuary (~106 km long) is the seaward end of Loire River, a major European river, with a mean annual waterflow of 890 $m^3\ s^{-1}$. The well mixed and highly turbid sedimentary plume of this estuary extends over a large part of the northern Bay of Biscay continental shelf (Dulaquais et al., 2020) (Waeles et al. 2004). The maximum turbidity zone (MTZ), delimited where SPM in the water column water reach > 1g L^{-1}, is estimated to be about 20- to 50-km long (Briant et al., 2021; Dulaquais et al., 2020; Jalón-Rojas et al., 2016). The Loire estuary has an industrialized and urbanized watershed that comprises the metropolitan areas of Nantes and Saint-Nazaire with its more than 800,000 inhabitants (Grosbois et al., 2012; Coynel et al., 2016).

A previous Cu isotope characterization of surface and core sediments in this estuary indicated a dominant natural Cu origin and a spatial isotope variability related to the hydrodynamic particle sorting between silt, clay, organic and amorphous particles through the fluvial-estuarine continuum (Araújo et al., 2019b). In turn, Zn isotope compositions in this zone was explained by natural and anthropogenic mixing source processes (Araújo et al., 2019). A similar explanation was also proposed for the variations observed in oysters (*Crassostrea gigas*) harvested near this estuary (Araújo et al., 2021).

For this study, the SPM samples near the Loire estuary were collected in April 2013 at 2 stations in the north Bay of Biscay inner shelf (LEP1 and LEP2). Sampling was performed by successive horizontal trawls using nylon nets (0.25 m^2 circular opening, 63 µm mesh size) coupled to a cylindric polymer collector at its end, in order to collect enough material in the 5 m below the surface for analyses. We thus considered contributions from remobilized particles from bottom sediments negligible.

At each station, seawater samples were collected through a WP2 sampling system and wet-sieved through a series of nylon sieves with mesh sizes of 2000, 1000, 500, 250 and 63 µm

previously cleaned with ultra-pure water in a containerized clean-room to prevent contamination. A total of four sub-samples representing the following size fractions were obtained for station LE1 south east of the river mouth (Fig. 1): >2000, 1000-500, 500-250, and 250-63 µm. The same fractions were chosen for station LE2 located north east of the river mouth, except 1000-500 µm, where insufficient amounts of material were collected to allow analyses. These size fractions are operationally defined and commonly used in the study of trace elements in marine plankton assemblages (e.g. Chouvelon et al., 2019; Strady et al., 2015). Several studies showed that size fractions >60 µm likely contain a greater fraction of (living) phyto- and/or zooplankton that mostly sustain higher trophic levels, and no more detritus, viro- or bacterioplankton (e.g. Rolff and Elmgren 2000, Espinasse et al. 2014).

Filtered seawater from the site was used to gently push SPM tangentially to the surface of the sieves. Then, SPM size fractions were poured in acid-cleaned polyethylene tubes and immediately frozen at -18°C. Back at the laboratory, they were freeze-dried and then stored at room temperature, in the dark in the laboratory until analyses. A total between 5 and 7 g of sample mass were obtained for each sampling station (Supplementary Material -Table 1S). For LE1, 57% of total mass concentrated in the 63-250 µm and 16% in 250-500 µm (Table 1S). For LE2, 63-250 and 250-500 µm contributed with 35 and 40% approximately. In both stations, the class 500-100 µm had few materials, below 5%.

As noted, the SPM was collected with plankton nets and sampling protocols designed to preserve as much as possible the integrity of organisms it may contain for later identification and quantification (Chouvelon et al., 2019). However, these methods normally result in complex samples that include both planktonic organisms and non-living organic and inorganic particles. Nevertheless, this method is advantageous as it preserves cellular contents of organisms and allows their concentration from tens of cubic meters of seawater. Indeed, for an example, frontal-flow filtration rapidly clogs and likely induces plasmatic membrane rupture. In this work, “SPM” designates the range of particle matrices present in the surface of an estuarine water column and collected using a plankton net and serial wet sieving.

2.2 Elemental and isotope analysis

Dry SPM samples were weighted in Teflon® reactor vessels and digested with nitric acid solution (3 ml of concentrated HNO_3 + 3 ml of H_2O) assisted by microwave radiation. This method extracts metals from potentially bioavailable phases, commonly referred as water-soluble, and also the exchangeable, acid-soluble, reducible, oxidable, etc. phases (Gleyzes et al., 2002; Rao et al., 2008; Tessier & Turner, 1995; Tonhá et al., 2021). It is considered a partial

extraction of the sample, and since hydrofluoric acid (HF) that breaks down crystalline matrices was not included, we consider negligible the fraction of extracted metals from crystal lattices of silicates. Splits from the final solution were subsequently analyzed for metal concentrations by ICP-MS (Cu, Zn, Pb, Cd, Ag, Co, Cr, Ni, Mn, Ti, V, Fe, and Al) and isotope compositions. Plankton BCR 414 and oyster soft tissue SRM 1566b, as reference materials (RMs) of biological matrices, were used since they are closest to the planktonic and marine characters of our samples. They were processed jointly with each sample batch, including procedural blanks, and recoveries are within ±10% of certified values. Similar recoveries were obtained for MESS-3 reference material (RM), digested using a total extraction (e.g., with HF, as described in Araújo et al., 2019a,b). The latter was used only for analytical control of isotopic analyses.

Cu and Zn were isolated from their matrix interferents before isotope analysis by ion exchange column chromatography packed with AG-MP1 resin following an adaptation of the protocol of Maréchal et al. (1999). Chromatographic recovery yields were checked by ICP-MS and isotope ratios measured by MC-ICP-MS (Neptune, Thermo Scientific) at the analytical platform (PSO *Pôle Spectrométrie Océan*, Ifremer, Brest, France). Samples dissolved in 2% (v/v) HNO_3 medium at metal concentrations of 250 ng.ml^{-1} were introduced using a stable introduction system and mass bias corrected by a combination of a sample-standard bracketing combined with external normalization technique (Cu doping Zn samples and vice-versa). The Cu and Zn isotope compositions of samples are expressed as δ^{65}Cu and δ^{66}Zn values, using the NIST SRM 976 and the "JMC-Lyon" as reference standards according to Equations 1 and 2, respectively:

$$\delta^{65}Cu_{SRM-976}\ (‰) = \left(\frac{R\left(\frac{^{65}Cu}{^{63}Cu}\right)_{sample}}{R\left(\frac{^{65}Cu}{^{63}Cu}\right)_{SRM-976}} - 1 \right) x\ 1000 \quad \text{(Eq.1)}$$

$$\delta^{66}Zn_{JMC-Lyon}\ (‰) = \left(\frac{R\left(\frac{^{66}Zn}{^{64}Zn}\right)_{sample}}{R\left(\frac{^{66}Zn}{^{64}Zn}\right)_{JMC-Lyon}} - 1 \right) x\ 1000 \quad \text{(Eq. 2)}$$

The average precision (2s) obtained from two or three measurements for a single replicate during a unique analytical session was ±0.04‰ for both analytes. Our obtained $\delta^{65}Cu_{SRM-976}$ value for the plankton RM BCR 414 (-0.27 ± 0.02‰, 2s, n = 3) agreed with reported values in

literature (–0.29 ± 0.10‰, 2σ, n = 3, Yang et al., 2020; -0.27 ± 0.05‰, Takano et al., 2020), while the corresponding $\delta^{66}Zn_{JMC}$ for this RM (+0.23 ±0.09‰, 2s, n = 1) fell in the same range of values reported by Takano et al.(2020) of +0.31 ± 0.03‰ (2s, n = 10). Longer time series of analyses of the oyster tissue SRM 1566b yielded reproductible $\delta^{65}Cu_{SRM\text{-}976}$ and $\delta^{66}Zn_{JMC}$ values of +0.23 ±0.03‰ (2s, n = 11) and +0.70 ±0.05‰ (2s, n = 5), respectively. These values are close to the $\delta^{65}Cu_{SRM\text{-}976}$ value of +0.30 ±0.02 (2s, n= 4, Jeong et al., 2021) and $\delta^{66}Zn_{JMC}$ values of +0.68 ± 0.04‰ (n= 14, 2s, Nitzsche et al., 2021). Measurements of the sediment MESS-3 RM during several analytical sessions yielded a $\delta^{66}Zn_{JMC}$ of +0.26 ± 0.06‰ (2s, n= 9), which agrees with another published value (+0.28 ± 0.02‰ , 2s, n= 4, Druce et al., 2020). The corresponding $\delta^{65}Cu_{SRM\text{-}976}$ for this sediment was +0.03 ±0.1 (n= 9), but no literature data are available for comparison.

2.3 Principal Component Analysis (PCA)

Principal Component Analysis (PCA) was applied to identify the main interrelations among the elemental variables, and hence, summarizing dataset information by grouping inter-correlated variables in principal components (Meglen, 1992). PCA factor loads were calculated using the correlation matrix with varimax rotation. The principal components (PCs) that had eigenvalues higher than 1 were selected for discussion (Mar da Costa et al., 2016; Mulholland et al., 2012). The communalities values of all variables equal or higher than 0.5 were used as thresholds for PCA results acceptance (Araújo, et al., 2019). PCA analysis was performed using the SPSS® software v.18.0 (IBM®). Linear relationship between variables were estimated using Pearson coefficients.

3. Results and discussion

3.1 Elemental and isotope distributions in the SPM sub-fractions

Concentrations of Cu vary from 2 to 57 µg g^{-1} dry weight (dw) and display an overall tendency of increasing with decreasing particle size (Table 1; Fig. 2a,b). In turn, Zn concentrations range from 66 to 200 µg g^{-1} dw and are uncorrelated with particle size, with the highest Zn concentrations observed in intermediate-size fractions (Table 1; Fig. 2c,d). The $\delta^{65}Cu_{SRM\text{-}976}$ values of both sampling stations range from -0.45 to +0.51‰, while $\delta^{66}Zn_{JMC}$ values vary from +0.14 to +0.76‰. For both sites, the elemental and isotope Cu systematics demonstrate a clear trend towards lighter Cu isotope compositions and higher concentrations with smaller particle sizes (Fig. 2a,b). Zinc stable isotope systematics are less clear (Fig. 2c,d), even if the lightest

isotope compositions occur in the smallest size class 63-250 µm that was collected at both sampling stations, and in the 250-500 µm class of the LE2 sample. A comparison of particle classes of the same sizes shows similar values at both sites, except for Zn in the class size 250-500 µm.

Principal Component Analysis (PCA) was applied to the dataset to visualize the intercorrelations between the concentrations of Cu and Zn and other elements. It yields two main components that together explained 92% of total dataset variance and discriminated two clusters of elements, here labelled as "Group A" and "Group B", respectively (Fig. 3a). Group A comprises Cu, Pb, Ni, Cr, Co, Mn, V, Ti, Al and Fe, while Group B includes Zn, Cd, and Ag (Fig. 3a). Elements from the first cluster show an overall tendency of concentration increase with particle size decrease, analogous to Cu (Table 1). In the second cluster, the elements display highest concentrations in intermediate size fractions, similarly to Zn (Table 1). In Group A, major elements (Al and Fe) and trace elements (Mn, V, Ti, Co, Cr, V, Pb, and Ni) showed strong coefficients of correlations ($r > 0.9$, $p < 0.01$), while in Group B, Cd and Ag are strongly correlated among them ($r > 0.9$, $p < 0.01$). Copper show affinities with Cr and Ni ($0.7 < r < 0.9$, $p < 0.05$). In turn, Zn is not significantly correlated to Cd and Ag ($0.1 < p > 0.05$), despite belonging in the same cluster.

In the southernmost LE1 sampling station, the finer SPM sub-fraction of 63-250 µm contribute with 73% of total Cu mass. Based on the mass sub-fractions and their respective Cu concentrations we estimate a bulk SPM concentration of 13 µg g^{-1} and a $\delta^{65}Cu$ value near -0.27‰ (Table 1S). This estimated isotope value is much lighter than the average obtained for the bottom sediments from the Loire estuary mouth and its vicinities (–0.04 ± 0.18, 2s, n=31, Araújo et al., 2019b). For Zn, estimations yield a concentration of 96 µg g^{-1} and a $\delta^{66}Zn$ value of +0.43‰, which fell above the average of the local sedimentary surface (+0.24 ±0.06, 2s, n=25). The difference between bulk SPM and bottom sediments suggest differences in their physicochemical compositions of each compartment. Surface sediments tend to be enriched in denser particles that settled through the water-column and their composition modified by early diagenesis occurring immediately below.(Coynel et al., 2016; Dang, et al., 2015). An unfortunately missing analysis of the (1000-500 µm) fractions did not allow to estimate bulk values at LE2.

3.2 Using Cu isotope information to infer particle origins and underlying processes

The northern continental shelf Bay of Biscay receives high loads of metals associated with i) inorganic and organic particles derived from weathering and erosion of the continental surface,

ii) in situ primary productivity, and iii) anthropogenic emissions from the Loire estuary watershed (Araújo, et al., 2019b; Briant et al., 2017, 2021; Coynel et al., 2016; Penaud et al., 2020). This particulate material is likely the main source of the elements from group "A" in the PCA analysis (Cu, Al, Fe, Mn, V, Cr, Ni, Ti, Pb, Co). The similar Fe to Al ratio in all the SPM samples indicates that the relative proportions of these two major elements are constant across the different particle size classes (Fig. 3b), which demonstrates that terrigenous materials are ubiquitous in the samples. Figure 3b also shows that, increased Fe and Al concentrations with decreasing particle size indicates a stronger imprint of "continental" inorganic (i.e., Fe and Al-containing) particles on the smaller size class particles (Fig. 3b). The accompanying concentration of the "continental" trace elements (group "A"), including Cu, point to the role of geogenic particles, mostly composed of clay minerals and their surface coatings, in transporting these elements from estuary mouth to the shelf of the bay.

The observed lighter Cu isotope compositions of finer particles are also consistent with the presence of weathered, smaller-size minerals and their increased capacity to adsorb this trace metal. In the critical zone, once released from their primary mineral structures, Cu isotopes tend to partition between aqueous organic complexes and residual particulate phases (Fe-Mn oxyhydroxides, clay minerals). The former become enriched with the heavy isotopes, while the latter become enriched with the light isotopes (Little et al., 2014; Vance et al., 2016). Field studies observed the link between enrichment of light isotopes in clay minerals with primary mineral depletion in soils (Guinoiseau et al., 2017, 2018b), while batch experiments showed the preferential light isotope adsorption on the surface of kaolinite (Li et al., 2015), and preferential heavy isotope losses in acid-leachates on natural basalts (Li & Liu, 2022). The coherence of our results with the cited field and laboratory studies point to weathering as the primary source of Cu with cumulative effects of organic ligands adsorption on solid surfaces as the principal controlling processes of group "A" (continental) elements in the finer particle size classes.

Conversely, the coarser SPM fractions exhibit lower concentration of crustal elements (Table 1), and hence, we infer that the relative fraction of organic matter, which includes living organisms and detrital forms of plants and micro-organisms, should increase. It is well known that Cu presents high affinity with organic matter (Ilina et al., 2013). Furthermore, experimental adsorption of Cu isotopes on organic matter (insolubilized humic acid-IHA) indicates the preferential retention of the heavy isotope in the organo-Cu complexes (Bigalke et al., 2010). Similarly, Cu adsorption onto phototrophic biofilm induces enrichment of biomass in heavy isotope (Coutaud et al., 2014). These observations suggest that Cu-organic matter-associations

304 in the SPM fractions could form a pool of isotopically heavy Cu. Indeed, the homeostatic
305 regulation of Cu in microorganisms, such as in meso- and macro-plankton could result in an
306 isotopically heavy, bioaccumulated Cu pool. It is well-know that Cu heavy isotopes
307 preferentially tend to bound to O- and N- donors of proteins involved in metabolic functions
308 (Albarède et al., 2016). Conversely, light Cu isotopes would be preferentially associated to S-
309 ligands often used for detoxification and excretion processes. High positive δ^{65}Cu values found
310 in sheep and mouse kidney has been also interpreted in terms of isotope fractionation in redox
311 reactions involving Cu (I) and Cu (II) species. These dual and opposite effects fractionation
312 mechanisms were also used to explain Cu isotope systematic observed in mussels (Araújo, et
313 al., 2021). It is unknown if the plankton of distinct size classes, composed of different species
314 assemblages present different isotope enrichment patterns related to metabolic and homeostatic
315 processes. In any case, the Cu isotope systematic presented here identifies two main Cu pools
316 in suspended particulate matter: a mineral rich (continental) pool, enriched in light isotopes,
317 and an organic-rich, labile pool, enriched in the heavy isotope. Such a systematic is very similar
318 to the particulate phase of South Atlantic ocean waters (Little et al., 2018).
319
320 *3.3 Using Zn isotope composition to infer particle origins and underlying processes*
321 The inter-correlations among Cd, Zn, and Ag identified in PCA analysis suggest that these
322 elements are less influenced by the detrital, terrigenous materials that are preferentially present
323 in the smaller-size SPM sub-fractions. Their concentrations and mass contents do not increase
324 with decreasing particulate size. Rather, they tend to be highest in intermediate size fractions
325 of SPM (Fig. 2c,d, for Zn; Table 1, for Ag and Cd). A similar pattern was also reported, but not
326 explained, in another study conducted in Gulf of Lions (NW Mediterranean Sea, Chouvelon et
327 al., 2019) using an analogous sample preparation, that is, seawater passed through sieves of
328 decreasing mesh (200, 60 and 6 µm). The authors related the observed Cd, Zn and Ag
329 distributions in SPM sub-fractions to the assimilation of Zn, Cd and Ag by copepods via
330 protozoa diet (Chouvelon et al., 2019), despite the lack of detailed information about actual
331 species distribution in the various SPM fractions. Indeed, the literature shows biomagnification
332 of Zn, Cd and Ag in the low part of the trophic chain (Reinfelder et al. 1998). A higher Zn
333 association with biologically-influenced particles is consistent with its status as the second-
334 most abundant micronutrient in phytoplankton biomass (Morel, 2003; Twining & Baines,
335 2013).
336 The smallest size-classes of the SPM in LE1 (250-63 µm) and LE2 (500-250 µm and
337 250-63 and) displayed δ^{66}Zn values within the range for Loire estuary bottom sediments, about

+0.24 ± 0.11 (2s, *n*=26, Araújo et al., 2019). Zinc concentration of the surface sediment in the Loire estuary mouth is influenced by geogenic ($\delta^{66}Zn_{JMC}$ ~0.3‰) and anthropogenic Zn ($\delta^{66}Zn_{JMC}$ ~0.1‰). Thus, these natural and anthropic Zn sources may also be reflected in the Zn isotope compositions observed in the finer particle fractions of LE1 and LE2 sampling stations.

Overall, Zn isotope variability of smaller, geogenic particles is close to crustal rocks since isotope fractionation along weathering processes is small, but a subtle isotope fractionation with preferential allocation of the heavy and light isotope in particulate and dissolved phases is noticeable in most field samples (Desaulty & Petelet-Giraud, 2020; Guinoiseau et al., 2018b; Little et al., 2014; Moynier et al., 2017; Suhr et al., 2018; Vance et al., 2016). Like for Cu, geogenic Zn isotope signatures seems to result from the balance between complexation by organic ligands and sorption on solid surfaces in weathering processes.

It is important to note that, like models, laboratory work does not include the complexity and conditions of real systems, which may yield findings different than field observations. For example, Zn batch adsorption experiments have mostly demonstrated a preferential binding of the heavy isotope in surfaces of clay minerals and Fe-Mn-Al oxyhydroxides (Komárek et al., 2021). However, in estuaries (e.g., Gironde and Pearl Harbor), it has observed an unexpected preferential removal of the light Zn isotope from the dissolved fraction via sorption processes on surface particles through the maximum turbidity zones (Ma et al., 2020; Petit et al., 2015). The mismatch between field and laboratory results can also be related to equilibrium conditions built into experimental designs, whereas natural processes in dynamic areas close estuaries can occur kinetically-driven.

Anthropogenic Zn from urban and industrial emissions, mainly released by the erosion of Zn-plated materials, vehicular traffic (tires and brake pad wear, and combustion), and sewage has lighter isotope values centered around 0.1‰ (Desaulty & Petelet-Giraud, 2020; Nitzsche et al., 2021; Thapalia et al., 2015). Urban and industrial agglomerations close to estuaries represent several anthropogenic sources, and thus multi Zn emissions should occurs almost concomitantly (Barletta et al., 2019; Burt et al., 2019; Desaulty & Petelet-Giraud, 2020). Their mixing along the fluvial-estuarine continuum and in continental run-off makes pinpointing specific Zn sources challenging, generally requiring the combination of additional elemental and isotope source proxies (Gonzalez et al., 2016; Souto-Oliveira et al., 2019). Here, $\delta^{66}Zn$ values has been proved a good proxy to detect "Zn urban fingerprints" in the coastal environments (Zhang et al., 2018).

Nonetheless, the source mixing processes involving anthropogenic and geogenic Zn do not explain the heavier isotope enrichments (above 0.6‰) in the coarser fractions (> 250 µm in LE1 and > 500 µm in LE2). Such as inferred for Cu, a relative increase of a Zn-rich organic pool in the SPM coarser fractions should occur along with a decrease in the geogenic pool. Indeed, zinc associates with organic matter via physico-chemical reactions with organic solid surfaces of humic and fulvic acids, and with cell walls of living organisms, or with detrital material resulting of microbial degradation of plant or animal (Brown & Calas, 2011). Previous studies have argued that the scavenging of Zn from a marine water column onto organic particle surfaces favors the retention of heavier Zn isotopes in the particulate phase (Gélabert et al., 2006; John & Conway, 2014; Weber et al., 2018). This is coherent with the observed δ^{66}Zn distributions in vertical seawater profiles from the Atlantic and Pacific oceans (John et al., 2018). The isotope distribution pattern resulting from this open ocean process also seems to hold true for our study site on the continental shelf. There, in parallel to physico-chemical sorption processes, intracellular uptake of Zn can also occur favoring the light isotope enrichment in living cells via kinetically-driven isotope fractionation (Twining & Baines, 2013; Araújo et al., 2018; Caldelas et al., 2011; John et al., 2007; Köbberich & Vance, 2019). However, given the relatively high δ^{66}Zn values from biogenic particles, the hypothesis of cellular uptake seems to be a minor influence on the Zn isotope compositions in the studied sub-fractions.

3.4 Isotope identification of biogenic pools and their relevance for marine trophic web studies

For our samples, the previous sections suggested that biogenic pools predominate in coarser sub-fractions and have heavier isotope compositions than geogenic ones. Indeed, for Zn, as the biogenic pool increases in larger sized SPM sub-fractions, δ^{66}Zn values increase, approaching that of local filter-feeding organisms (oysters) (Fig. 4). The nearing SPM and biota isotope signatures suggest that the "biogenic Zn" pool from SPM is available for bioaccumulation in upper trophic levels via dietary intake, and therefore, does represent the local marine trophic baseline. Below are the main arguments in support of our suggestion that δ^{66}Zn isotope values in oysters are consistent with the hypothesis of a bioavailable biogenic Zn pool.

Oysters are filter-feeders capable of filtering large quantities of seawater to extract their sustenance from seston (e.g., phytoplankton and algae debris). (Dame, 2012; Gosling, 2003; Wang and Wang, 2019). Being primary consumers, the isotope composition of carbon and nitrogen in their tissues are reliable proxies to assess their organic dietary sources (Briant et al., 2018). Furthermore, they accumulate metals through both particulate and dissolved pathways.

405 The particulate phase is associated with the diet and is considered the main route of
406 bioaccumulation (Akcha et al., 2022; Griscom & Fisher, 2004). Oysters' ability to uptake
407 contaminants and especially metals in their tissues justifies their wide use for biomonitoring
408 marine environments. Recently, determinations of metal isotopes in oysters from biomonitoring
409 sample banks has inferred anthropogenic origins and bioaccumulation routes for these
410 elements. Since internal biological Zn fractionation of oysters does not affect the isotope record
411 of Zn sources, these organisms are a reliable proxy of the Zn to which they are exposed in the
412 surrounding medium (Ma et al., 2019; Ma & Wang, 2021). Therefore, Zn isotopes in the
413 temporal series of bivalves have helped reconstruct anthropogenic Zn bioaccumulation
414 tendencies in French estuaries (Araújo, et al., 2021).
415 Furthermore, in a spatial sampling of these organisms paired with SPM and water
416 samples from the Pearl Harbor estuary, (Ma et al., 2021) quantified relative fractions of Zn
417 bioaccumulated via dissolved and particulate routes, assuming that Zn from bulk SPM was
418 entirely bioavailable. This assumption, however, is not necessarily true in natural systems and
419 it may be necessary to refine uptake models for quantifying relative fractions contributions
420 more accurately. Indeed, selective extractions using organic solvents (e.g., isopropanol) in
421 continental margin sediments worldwide revealed that soluble organic fractions have heavier
422 Zn isotope compositions (>0.5‰ than the bulk material (~0.3‰) analyzed (Y. Zhang et al.,
423 2021). Like our samples, the prevalent heavy isotope in these organic factions has also been
424 associated with biological activity and scavenging processes. Interestingly, the heavy isotope
425 enrichment in biogenic materials seems coherent with organic-derived materials, such as
426 bituminous coal (~1.3‰, Gonzalez & Weiss, 2015). With oyster isotope records as a proxy of
427 bioavailable Zn, the all mentioned evidence supports our hypothesis that a biogenic pool
428 enriched in the heavy isotope is a primary Zn source for these organisms.
429
430 **4. Conclusions**
431 This study reports for the first-time the isotope compositions of Cu and Zn in different size
432 fractions of SPM (63-250; 250-500; 500-1000; and 1000-2000 µm) from a continental shelf.
433 These data showed significant isotope variability between particle size fractions greater than
434 that observed for bulk bottom sediment collected over the entire study site (e.g., for Zn, Fig. 4).
435 The Cu and Zn isotope systematics, combined with the elemental composition dataset, allowed
436 to distinguish two main Cu and Zn pools within the SPM. These pools control the behavior of
437 these elements: the (relatively) refractory geogenic pool is enriched in light isotopes, while the
438 (relatively) labile pool is enriched in heavy isotopes. Both pools are present in all SPM sub-

fractions, but their relative proportions vary according to particle size. The observed heavier isotope composition of biogenic particles likely reflects the local trophic marine baseline and explains the close isotope values observed in secondary consumers (i.e., oysters). We suggest that combining target-specific size classes and using selective extractions may improve the isotope characterization of different metal pools which may have different bioavailabilities. For bivalves, isotope characterization of metals in particles from the size range of food particles (1-10 µm, Gosling, 2003) is suggested, to enable source apportionment of bioaccumulation routes (dissolved *vs*. particulate).

This study confirms that isotope analyses in distinct class-sized particles can provide additional information related to host phases of Cu and Zn, and their entry at the base of the trophic food-web. For future studies on trace metals, we recommend combining mineralogical and plankton assemblages with speciation and isotope characterization. This information will allow to better understand the influence of particle composition on the input, dissolution, scavenging, (dis-)aggregation, and transport of these elements in the marine environment.

Acknowledgements

The authors would like to thanks all the entire team on board the R/V *Thalia* and everyone involved in the "Camelia" project (DOI: 10.18142/281). The authors are also deeply thankful for the thorough and constructive corrections and insightful comments from anonymous reviewers, which have substantially improved the initial manuscript.

References

Akcha, F., Coquillé, N., Sussarellu, R., Rouxel, J., Chouvelon, T., Gonzalez, P., Legeay, A., Bruzac, S., Sireau, T., Gonzalez, J.-L., Gourves, P.-Y., Godfrin, Y., Buchet, V., & Stachowski-Haberkorn, S. (2022). Trophic transfer of copper decreases the condition index in Crassostrea gigas spat in concomitance with a change in the microalgal fatty acid profile and enhanced oyster energy demand. *Science of The Total Environment*, *824*, 153841. https://doi.org/10.1016/j.scitotenv.2022.153841

Albarede, F., Télouk, P., Balter, V., Bondanese, V. P., Albalat, E., Oger, P., Bonaventura, P., Miossec, P., & Fujii, T. (2016). Medical applications of Cu, Zn, and S isotope effects. *Metallomics*, *8*(10), 1056–1070. https://doi.org/10.1039/C5MT00316D

Aranda, S., Borrok, D. M., Wanty, R. B., & Balistrieri, L. S. (2012). Zinc isotope investigation of surface and pore waters in a mountain watershed impacted by acid rock drainage. *Science of The Total Environment*, *420*, 202–213. https://doi.org/10.1016/j.scitotenv.2012.01.015

Araújo, D. F., Knoery, J., Briant, N., Vigier, N., & Ponzevera, E. (2022). "Non-traditional" stable isotopes applied to the study of trace metal contaminants in anthropized marine environments. *Marine Pollution Bulletin*, *175*, 113398. https://doi.org/10.1016/j.marpolbul.2022.113398

Araújo, D. F., Machado, W., Weiss, D., Mulholland, D. S., Garnier, J., Souto-Oliveira, C. E., & Babinski, M. (2018). Zinc isotopes as tracers of anthropogenic sources and biogeochemical processes in contaminated mangroves. *Applied Geochemistry*, *95*, 25–32. https://doi.org/10.1016/j.apgeochem.2018.05.008

Araújo, D. F., Ponzevera, E., Briant, N., Knoery, J., Bruzac, S., Sireau, T., & Brach-Papa, C. (2019). Copper, zinc and lead isotope signatures of sediments from a mediterranean coastal bay

impacted by naval activities and urban sources. *Applied Geochemistry*, *111*, 104440. https://doi.org/10.1016/j.apgeochem.2019.104440

Araújo, D. F., Ponzevera, E., Briant, N., Knoery, J., Bruzac, S., Sireau, T., Pellouin-Grouhel, A., & Brach-Papa, C. (2021). Differences in Copper Isotope Fractionation Between Mussels (Regulators) and Oysters (Hyperaccumulators): Insights from a Ten-Year Biomonitoring Study. *Environmental Science & Technology*, *55*(1), 324–330. https://doi.org/10.1021/acs.est.0c04691

Araújo, D. F., Ponzevera, E., Briant, N., Knoery, J., Sireau, T., Mojtahid, M., Metzger, E., & Brach-Papa, C. (2019). Assessment of the metal contamination evolution in the Loire estuary using Cu and Zn stable isotopes and geochemical data in sediments. *Marine Pollution Bulletin*, *143*, 12–23. https://doi.org/10.1016/j.marpolbul.2019.04.034

Araújo, D. F., Ponzevera, E., Weiss, D. J., Knoery, J., Briant, N., Yepez, S., Bruzac, S., Sireau, T., & Brach-Papa, C. (2021). Application of Zn Isotope Compositions in Oysters to Monitor and Quantify Anthropogenic Zn Bioaccumulation in Marine Environments over Four Decades: A "Mussel Watch Program" Upgrade. *ACS ES&T Water*, *1*(4), 1035–1046. https://doi.org/10.1021/acsestwater.1c00010

Araújo, D., Machado, W., Weiss, D., Mulholland, D. S., Boaventura, G. R., Viers, J., Garnier, J., Dantas, E. L., & Babinski, M. (2017). A critical examination of the possible application of zinc stable isotope ratios in bivalve mollusks and suspended particulate matter to trace zinc pollution in a tropical estuary. *Environmental Pollution*, *226*, 41–47. https://doi.org/10.1016/j.envpol.2017.04.011

Babcsányi, I., Chabaux, F., Granet, M., Meite, F., Payraudeau, S., Duplay, J., & Imfeld, G. (2016). Copper in soil fractions and runoff in a vineyard catchment: Insights from copper stable isotopes. *Science of The Total Environment*, *557–558*, 154–162. https://doi.org/10.1016/j.scitotenv.2016.03.037

Babcsányi, I., Imfeld, G., Granet, M., & Chabaux, F. (2014). Copper Stable Isotopes To Trace Copper Behavior in Wetland Systems. *Environmental Science & Technology*, *48*(10), 5520–5529. https://doi.org/10.1021/es405688v

Barletta, M., Lima, A. R. A., & Costa, M. F. (2019). Distribution, sources and consequences of nutrients, persistent organic pollutants, metals and microplastics in South American estuaries. *Science of The Total Environment*, *651*, 1199–1218. https://doi.org/10.1016/j.scitotenv.2018.09.276

Bianchi, T. S. (2007). *Biogeochemistry of estuaries*. Oxford University Press.

Bigalke, M., Weyer, S., & Wilcke, W. (2010). Copper Isotope Fractionation during Complexation with Insolubilized Humic Acid. *Environmental Science & Technology*, *44*(14), 5496–5502. https://doi.org/10.1021/es1017653

Borrok, D. M., Nimick, D. A., Wanty, R. B., & Ridley, W. I. (2008). Isotopic variations of dissolved copper and zinc in stream waters affected by historical mining. *Geochimica et Cosmochimica Acta*, *72*(2), 329–344. https://doi.org/10.1016/j.gca.2007.11.014

Briant, N., Chiffoleau, J.-F., Knoery, J., Araújo, D. F., Ponzevera, E., Crochet, S., Thomas, B., & Brach-Papa, C. (2021). Seasonal trace metal distribution, partition and fluxes in the temperate macrotidal Loire Estuary (France). *Estuarine, Coastal and Shelf Science*, *262*, 107616. https://doi.org/10.1016/j.ecss.2021.107616

Briant, N., Chouvelon, T., Martinez, L., Brach-Papa, C., Chiffoleau, J., Savoye, N., Sonke, J., & Knoery, J. (2017). Spatial and temporal distribution of mercury and methylmercury in bivalves from the French coastline. *Marine Pollution Bulletin*, *114*(2), 1096–1102. https://doi.org/10.1016/j.marpolbul.2016.10.018

Brown, G. E., & Calas, G. (2011). Environmental mineralogy – Understanding element behavior in ecosystems. *Comptes Rendus Geoscience*, *343*(2), 90–112. https://doi.org/10.1016/j.crte.2010.12.005

Burt, J. A., Killilea, M. E., & Ciprut, S. (2019). Coastal urbanization and environmental change: Opportunities for collaborative education across a global network university. *Regional Studies in Marine Science*, *26*, 100501. https://doi.org/10.1016/j.rsma.2019.100501

Caldelas, C., Dong, S., Araus, J. L., & Jakob Weiss, D. (2011). Zinc isotopic fractionation in Phragmites australis in response to toxic levels of zinc. *Journal of Experimental Botany*, *62*(6), 2169–2178. https://doi.org/10.1093/jxb/erq414

Chester, R. (2003). *Marine geochemistry* (2. ed). Blackwell Science.
Chouvelon, T., Strady, E., Harmelin-Vivien, M., Radakovitch, O., Brach-Papa, C., Crochet, S., Knoery, J., Rozuel, E., Thomas, B., Tronczynski, J., & Chiffoleau, J.-F. (2019). Patterns of trace metal bioaccumulation and trophic transfer in a phytoplankton-zooplankton-small pelagic fish marine food web. *Marine Pollution Bulletin*, *146*, 1013–1030. https://doi.org/10.1016/j.marpolbul.2019.07.047
Coutaud, A., Meheut, M., Viers, J., Rols, J.-L., & Pokrovsky, O. S. (2014). Zn isotope fractionation during interaction with phototrophic biofilm. *Chemical Geology*, *390*, 46–60. https://doi.org/10.1016/j.chemgeo.2014.10.004
Coynel, A., Gorse, L., Curti, C., Schafer, J., Grosbois, C., Morelli, G., Ducassou, E., Blanc, G., Maillet, G. M., & Mojtahid, M. (2016). Spatial distribution of trace elements in the surface sediments of a major European estuary (Loire Estuary, France): Source identification and evaluation of anthropogenic contribution. *Journal of Sea Research*, *118*, 77–91. https://doi.org/10.1016/j.seares.2016.08.005
Dang, D. H., Lenoble, V., Durrieu, G., Omanović, D., Mullot, J.-U., Mounier, S., & Garnier, C. (2015). Seasonal variations of coastal sedimentary trace metals cycling: Insight on the effect of manganese and iron (oxy)hydroxides, sulphide and organic matter. *Marine Pollution Bulletin*, *92*(1–2), 113–124. https://doi.org/10.1016/j.marpolbul.2014.12.048
Dang, D. H., Schäfer, J., Brach-Papa, C., Lenoble, V., Durrieu, G., Dutruch, L., Chiffoleau, J.-F., Gonzalez, J.-L., Blanc, G., Mullot, J.-U., Mounier, S., & Garnier, C. (2015). Evidencing the Impact of Coastal Contaminated Sediments on Mussels Through Pb Stable Isotopes Composition. *Environmental Science & Technology*, *49*(19), 11438–11448. https://doi.org/10.1021/acs.est.5b01893
de Souza Machado, A. A., Spencer, K., Kloas, W., Toffolon, M., & Zarfl, C. (2016). Metal fate and effects in estuaries: A review and conceptual model for better understanding of toxicity. *Science of The Total Environment*, *541*, 268–281. https://doi.org/10.1016/j.scitotenv.2015.09.045
Dekov, V. M., Vanlierde, E., Billström, K., Garbe-Schönberg, C.-D., Weiss, D. J., Gatto Rotondo, G., Van Meel, K., Kuzmann, E., Fortin, D., Darchuk, L., & Van Grieken, R. (2014). Ferrihydrite precipitation in groundwater-fed river systems (Nete and Demer river basins, Belgium): Insights from a combined Fe-Zn-Sr-Nd-Pb-isotope study. *Chemical Geology*, *386*, 1–15. https://doi.org/10.1016/j.chemgeo.2014.07.023
Desaulty, A.-M., & Petelet-Giraud, E. (2020). Zinc isotope composition as a tool for tracing sources and fate of metal contaminants in rivers. *Science of The Total Environment*, *728*, 138599. https://doi.org/10.1016/j.scitotenv.2020.138599
Druce, M., Stirling, C. H., & Rolison, J. M. (2020). High-Precision Zinc Isotopic Measurement of Certified Reference Materials Relevant to the Environmental, Earth, Planetary and Biomedical Sciences. *Geostandards and Geoanalytical Research*, *44*(4), 711–732. https://doi.org/10.1111/ggr.12341
Ducher, M., Blanchard, M., & Balan, E. (2016). Equilibrium zinc isotope fractionation in Zn-bearing minerals from first-principles calculations. *Chemical Geology*, *443*, 87–96. https://doi.org/10.1016/j.chemgeo.2016.09.016
Dulaquais, G., Waeles, M., Breitenstein, J., Knoery, J., & Riso, R. (2020). Links between size fractionation, chemical speciation of dissolved copper and chemical speciation of dissolved organic matter in the Loire estuary. *Environmental Chemistry*, *17*(5), 385. https://doi.org/10.1071/EN19137
El Azzi, D., Viers, J., Guiresse, M., Probst, A., Aubert, D., Caparros, J., Charles, F., Guizien, K., & Probst, J. L. (2013). Origin and fate of copper in a small Mediterranean vineyard catchment: New insights from combined chemical extraction and δ65Cu isotopic composition. *Science of The Total Environment*, *463–464*, 91–101. https://doi.org/10.1016/j.scitotenv.2013.05.058
Fujii, T., Moynier, F., Blichert-Toft, J., & Albarède, F. (2014). Density functional theory estimation of isotope fractionation of Fe, Ni, Cu, and Zn among species relevant to geochemical and biological environments. *Geochimica et Cosmochimica Acta*, *140*, 553–576. https://doi.org/10.1016/j.gca.2014.05.051
Gélabert, A., Pokrovsky, O. S., Viers, J., Schott, J., Boudou, A., & Feurtet-Mazel, A. (2006). Interaction between zinc and freshwater and marine diatom species: Surface complexation and

Zn isotope fractionation. *Geochimica et Cosmochimica Acta*, *70*(4), 839–857. https://doi.org/10.1016/j.gca.2005.10.026
Gleyzes, C., Tellier, S., & Astruc, M. (2002). Fractionation studies of trace elements in contaminated soils and sediments: A review of sequential extraction procedures. *TrAC Trends in Analytical Chemistry*, *21*(6), 451–467. https://doi.org/10.1016/S0165-9936(02)00603-9
Gonzalez, R. O., Strekopytov, S., Amato, F., Querol, X., Reche, C., & Weiss, D. (2016). New Insights from Zinc and Copper Isotopic Compositions into the Sources of Atmospheric Particulate Matter from Two Major European Cities. *Environmental Science & Technology*, *50*(18), 9816–9824. https://doi.org/10.1021/acs.est.6b00863
Gonzalez, R., & Weiss, D. (2015). Zinc Isotope Variability in Three Coal-Fired Power Plants: A Predictive Model for Determining Isotopic Fractionation during Combustion. *Environmental Science & Technology*, *49*(20), 12560–12567. https://doi.org/10.1021/acs.est.5b02402
Gosling, E. M. (2003). *Bivalve molluscs: Biology, ecology, and culture*. Fishing News Books.
Griscom, S. B., & Fisher, N. S. (2004). Bioavailability of sediment-bound metals to marine bivalve molluscs: An overview. *Estuaries*, *27*(5), 826–838. https://doi.org/10.1007/BF02912044
Guinoiseau, D., Bouchez, J., Gélabert, A., Louvat, P., Moreira-Turcq, P., Filizola, N., & Benedetti, M. F. (2018a). Fate of particulate copper and zinc isotopes at the Solimões-Negro river confluence, Amazon Basin, Brazil. *Chemical Geology*, *489*, 1–15. https://doi.org/10.1016/j.chemgeo.2018.05.004
Guinoiseau, D., Bouchez, J., Gélabert, A., Louvat, P., Moreira-Turcq, P., Filizola, N., & Benedetti, M. F. (2018b). Fate of particulate copper and zinc isotopes at the Solimões-Negro river confluence, Amazon Basin, Brazil. *Chemical Geology*, *489*, 1–15. https://doi.org/10.1016/j.chemgeo.2018.05.004
Guinoiseau, D., Gélabert, A., Allard, T., Louvat, P., Moreira-Turcq, P., & Benedetti, M. F. (2017). Zinc and copper behaviour at the soil-river interface: New insights by Zn and Cu isotopes in the organic-rich Rio Negro basin. *Geochimica et Cosmochimica Acta*, *213*, 178–197. https://doi.org/10.1016/j.gca.2017.06.030
Ilina, S. M., Viers, J., Lapitsky, S. A., Mialle, S., Mavromatis, V., Chmeleff, J., Brunet, P., Alekhin, Y. V., Isnard, H., & Pokrovsky, O. S. (2013). Stable (Cu, Mg) and radiogenic (Sr, Nd) isotope fractionation in colloids of boreal organic-rich waters. *Chemical Geology*, *342*, 63–75. https://doi.org/10.1016/j.chemgeo.2013.01.019
Jalón-Rojas, I., Schmidt, S., Sottolichio, A., & Bertier, C. (2016). Tracking the turbidity maximum zone in the Loire Estuary (France) based on a long-term, high-resolution and high-frequency monitoring network. *Continental Shelf Research*, *117*, 1–11. https://doi.org/10.1016/j.csr.2016.01.017
Jeong, H., Ra, K., & Choi, J. Y. (2021). Copper, Zinc and Lead Isotopic Delta Values and Isotope Ratios of Various Geological and Biological Reference Materials. *Geostandards and Geoanalytical Research*, *45*(3), 551–563. https://doi.org/10.1111/ggr.12379
John, S. G., & Conway, T. M. (2014). A role for scavenging in the marine biogeochemical cycling of zinc and zinc isotopes. *Earth and Planetary Science Letters*, *394*, 159–167. https://doi.org/10.1016/j.epsl.2014.02.053
John, S. G., Geis, R. W., Saito, M. A., & Boyle, E. A. (2007). Zinc isotope fractionation during high-affinity and low-affinity zinc transport by the marine diatom *Thalassiosira oceanica*. *Limnology and Oceanography*, *52*(6), 2710–2714. https://doi.org/10.4319/lo.2007.52.6.2710
John, S. G., Helgoe, J., & Townsend, E. (2018). Biogeochemical cycling of Zn and Cd and their stable isotopes in the Eastern Tropical South Pacific. *Marine Chemistry*, *201*, 256–262. https://doi.org/10.1016/j.marchem.2017.06.001
Köbberich, M., & Vance, D. (2018). Zinc association with surface-bound iron-hydroxides on cultured marine diatoms: A zinc stable isotope perspective. *Marine Chemistry*, *202*, 1–11. https://doi.org/10.1016/j.marchem.2018.01.002
Köbberich, M., & Vance, D. (2019). Zn isotope fractionation during uptake into marine phytoplankton: Implications for oceanic zinc isotopes. *Chemical Geology*, *523*, 154–161. https://doi.org/10.1016/j.chemgeo.2019.04.004
Komárek, M., Ratié, G., Vaňková, Z., Šípková, A., & Chrastný, V. (2021). Metal isotope complexation with environmentally relevant surfaces: Opening the isotope fractionation black

box. *Critical Reviews in Environmental Science and Technology*, *0*(0), 1–31. https://doi.org/10.1080/10643389.2021.1955601

Lam, P. J., Lee, J.-M., Heller, M. I., Mehic, S., Xiang, Y., & Bates, N. R. (2018). Size-fractionated distributions of suspended particle concentration and major phase composition from the U.S. GEOTRACES Eastern Pacific Zonal Transect (GP16). *Marine Chemistry*, *201*, 90–107. https://doi.org/10.1016/j.marchem.2017.08.013

Lazure, P., Dumas, F., & Vrignaud, C. (2008). Circulation on the Armorican shelf (Bay of Biscay) in autumn. *Journal of Marine Systems*, *72*(1), 218–237. https://doi.org/10.1016/j.jmarsys.2007.09.011

Lazure, P., & Jegou, A.-M. (1998). 3D modelling of seasonal evolution of Loire and Gironde plumes on Biscay Bay continental shelf. *Oceanologica Acta*, *21*(2), 165–177. https://doi.org/10.1016/S0399-1784(98)80006-6

Li, D., & Liu, S.-A. (2022). Copper Isotope Fractionation during Basalt Leaching at 25 °C and pH = 0.3, 2. *Journal of Earth Science*, *33*(1), 82–91. https://doi.org/10.1007/s12583-021-1499-7

Li, D., Liu, S.-A., & Li, S. (2015). Copper isotope fractionation during adsorption onto kaolinite: Experimental approach and applications. *Chemical Geology*, *396*, 74–82. https://doi.org/10.1016/j.chemgeo.2014.12.020

Liang, L., Liu, C.-Q., Zhu, X., Ngwenya, B. T., Wang, Z., Song, L., & Li, J. (2020). Zinc Isotope Characteristics in the Biogeochemical Cycle as Revealed by Analysis of Suspended Particulate Matter (SPM) in Aha Lake and Hongfeng Lake, Guizhou, China. *Journal of Earth Science*, *31*(1), 126–140. https://doi.org/10.1007/s12583-017-0957-8

Little, S. H., Archer, C., Milne, A., Schlosser, C., Achterberg, E. P., Lohan, M. C., & Vance, D. (2018). Paired dissolved and particulate phase Cu isotope distributions in the South Atlantic. *Chemical Geology*, *502*, 29–43. https://doi.org/10.1016/j.chemgeo.2018.07.022

Little, S. H., Vance, D., Walker-Brown, C., & Landing, W. M. (2014). The oceanic mass balance of copper and zinc isotopes, investigated by analysis of their inputs, and outputs to ferromanganese oxide sediments. *Geochimica et Cosmochimica Acta*, *125*, 673–693. https://doi.org/10.1016/j.gca.2013.07.046

Ma, L., Li, Y., Wang, W., Weng, N., Evans, R. D., & Wang, W.-X. (2019). Zn Isotope Fractionation in the Oyster *Crassostrea hongkongensis* and Implications for Contaminant Source Tracking. *Environmental Science & Technology*, *53*(11), 6402–6409. https://doi.org/10.1021/acs.est.8b06855

Ma, L., Wang, W., Xie, M.-W., Wang, W.-X., & Evans, R. D. (2020). Using Zn Isotopic Signatures for Source Identification in a Contaminated Estuary of Southern China. *Environmental Science & Technology*, *54*(8), 5140–5149. https://doi.org/10.1021/acs.est.9b05955

Ma, L., & Wang, W.-X. (2021). Zinc source differentiation in hydrothermal vent mollusks: Insight from Zn isotope ratios. *Science of The Total Environment*, *773*, 145653. https://doi.org/10.1016/j.scitotenv.2021.145653

Ma, L., Wang, W.-X., & Evans, R. D. (2021). Distinguishing multiple Zn sources in oysters in a complex estuarine system using Zn isotope ratio signatures. *Environmental Pollution*, *289*, 117941. https://doi.org/10.1016/j.envpol.2021.117941

Mason, R. P. (2013). *Trace Metals in Aquatic Systems: Mason/Trace Metals in Aquatic Systems*. John Wiley & Sons, Ltd. https://doi.org/10.1002/9781118274576

Meglen, R. R. (1992). Examining large databases: A chemometric approach using principal component analysis. *Marine Chemistry*, *39*(1–3), 217–237. https://doi.org/10.1016/0304-4203(92)90103-H

Morel, F. M. M. (2003). The Biogeochemical Cycles of Trace Metals in the Oceans. *Science*, *300*(5621), 944–947. https://doi.org/10.1126/science.1083545

Moynier, F., Vance, D., Fujii, T., & Savage, P. (2017). The Isotope Geochemistry of Zinc and Copper. *Reviews in Mineralogy and Geochemistry*, *82*(1), 543–600. https://doi.org/10.2138/rmg.2017.82.13

Nitzsche, K. N., Yoshimura, T., Ishikawa, N. F., Ogawa, N. O., Suzuki, K., & Ohkouchi, N. (2021). Trace metal geochemical and Zn stable isotope data as tracers for anthropogenic metal contributions in a sediment core from Lake Biwa, Japan. *Applied Geochemistry*, *134*, 105107. https://doi.org/10.1016/j.apgeochem.2021.105107

Peel, K., Weiss, D., & Siggc, L. (2009). Zinc isotope composition of settling particles as a proxy for biogeochemical processes in lakes: Insights from the eutrophic Lake Greifen, Switzerland. *Limnology and Oceanography*, *54*(5), 1699–1708. https://doi.org/10.4319/lo.2009.54.5.1699

Penaud, A., Ganne, A., Eynaud, F., Lambert, C., Coste, P. O., Herlédan, M., Vidal, M., Goslin, J., Stéphan, P., Charria, G., Pailler, Y., Durand, M., Zumaque, J., & Mojtahid, M. (2020). Oceanic versus continental influences over the last 7 kyrs from a mid-shelf record in the northern Bay of Biscay (NE Atlantic). *Quaternary Science Reviews*, *229*, 106135. https://doi.org/10.1016/j.quascirev.2019.106135

Petit, J. C. J., Schäfer, J., Coynel, A., Blanc, G., Chiffoleau, J.-F., Auger, D., Bossy, C., Derriennic, H., Mikolaczyk, M., Dutruch, L., & Mattielli, N. (2015). The estuarine geochemical reactivity of Zn isotopes and its relevance for the biomonitoring of anthropogenic Zn and Cd contaminations from metallurgical activities: Example of the Gironde fluvial-estuarine system, France. *Geochimica et Cosmochimica Acta*, *170*, 108–125. https://doi.org/10.1016/j.gca.2015.08.004

Petit, J. C. J., Schäfer, J., Coynel, A., Blanc, G., Deycard, V. N., Derriennic, H., Lanceleur, L., Dutruch, L., Bossy, C., & Mattielli, N. (2013). Anthropogenic sources and biogeochemical reactivity of particulate and dissolved Cu isotopes in the turbidity gradient of the Garonne River (France). *Chemical Geology*, *359*, 125–135. https://doi.org/10.1016/j.chemgeo.2013.09.019

Rao, C. R. M., Sahuquillo, A., & Lopez Sanchez, J. F. (2008). A Review of the Different Methods Applied in Environmental Geochemistry For Single and Sequential Extraction of Trace Elements in Soils and Related Materials. *Water, Air, and Soil Pollution*, *189*(1), 291–333. https://doi.org/10.1007/s11270-007-9564-0

Schleicher, N. J., Dong, S., Packman, H., Little, S. H., Ochoa Gonzalez, R., Najorka, J., Sun, Y., & Weiss, D. J. (2020). A Global Assessment of Copper, Zinc, and Lead Isotopes in Mineral Dust Sources and Aerosols. *Frontiers in Earth Science*, *8*. https://doi.org/10.3389/feart.2020.00167

Schulz, H. D., & Zabel, M. (Eds.). (2006). *Marine Geochemistry*. Springer-Verlag. https://doi.org/10.1007/3-540-32144-6

Sherman, D. M., & Little, S. H. (2020). Isotopic disequilibrium of Cu in marine ferromanganese crusts: Evidence from ab initio predictions of Cu isotope fractionation on sorption to birnessite. *Earth and Planetary Science Letters*, *549*, 116540. https://doi.org/10.1016/j.epsl.2020.116540

Skierszkan, E. K., Mayer, K. U., Weis, D., & Beckie, R. D. (2016). Molybdenum and zinc stable isotope variation in mining waste rock drainage and waste rock at the Antamina mine, Peru. *Science of The Total Environment*, *550*, 103–113. https://doi.org/10.1016/j.scitotenv.2016.01.053

Souto-Oliveira, C. E., Babinski, M., Araújo, D. F., Weiss, D. J., & Ruiz, I. R. (2019). Multi-isotope approach of Pb, Cu and Zn in urban aerosols and anthropogenic sources improves tracing of the atmospheric pollutant sources in megacities. *Atmospheric Environment*, *198*, 427–437. https://doi.org/10.1016/j.atmosenv.2018.11.007

Sparks, D. L. (2005). Toxic Metals in the Environment: The Role of Surfaces. *Elements*, *1*(4), 193–197. https://doi.org/10.2113/gselements.1.4.193

Strady, E., Harmelin-Vivien, M., Chiffoleau, J. F., Veron, A., Tronczynski, J., & Radakovitch, O. (2015). 210Po and 210Pb trophic transfer within the phytoplankton–zooplankton–anchovy/sardine food web: A case study from the Gulf of Lion (NW Mediterranean Sea). *Journal of Environmental Radioactivity*, *143*, 141–151. https://doi.org/10.1016/j.jenvrad.2015.02.019

Suhr, N., Schoenberg, R., Chew, D., Rosca, C., Widdowson, M., & Kamber, B. S. (2018). Elemental and isotopic behaviour of Zn in Deccan basalt weathering profiles: Chemical weathering from bedrock to laterite and links to Zn deficiency in tropical soils. *Science of The Total Environment*, *619–620*, 1451–1463. https://doi.org/10.1016/j.scitotenv.2017.11.112

Takano, S., Liao, W.-H., Tian, H.-A., Huang, K.-F., Ho, T.-Y., & Sohrin, Y. (2020). Sources of particulate Ni and Cu in the water column of the northern South China Sea: Evidence from elemental and isotope ratios in aerosols and sinking particles. *Marine Chemistry*, *219*, 103751. https://doi.org/10.1016/j.marchem.2020.103751

Tessier, A., & Turner, D. R. (Eds.). (1995). *Metal speciation and bioavailability in aquatic systems*. J. Wiley.

Thapalia, A., Borrok, D. M., Van Metre, P. C., & Wilson, J. (2015). Zinc Isotopic Signatures in Eight Lake Sediment Cores from Across the United States. *Environmental Science & Technology*, *49*(1), 132–140. https://doi.org/10.1021/es5036893

Tonhá, M. S., Araújo, D. F., Araújo, R., Cunha, B. C. A., Machado, W., Portela, J. F., PR Souza, J., Carvalho, H. K., Dantas, E. L., Roig, H. L., Seyler, P., & Garnier, J. (2021). Trace metal dynamics in an industrialized Brazilian river: A combined application of Zn isotopes, geochemical partitioning, and multivariate statistics. *Journal of Environmental Sciences*, *101*, 313–325. https://doi.org/10.1016/j.jes.2020.08.027

Tonhá, M. S., Garnier, J., Araújo, D. F., Cunha, B. C. A., Machado, W., Dantas, E., Araújo, R., Kutter, V. T., Bonnet, M.-P., & Seyler, P. (2020). Behavior of metallurgical zinc contamination in coastal environments: A survey of Zn from electroplating wastes and partitioning in sediments. *Science of The Total Environment*, 140610. https://doi.org/10.1016/j.scitotenv.2020.140610

Turner, A., & Millward, G. E. (2002). Suspended Particles: Their Role in Estuarine Biogeochemical Cycles. *Estuarine, Coastal and Shelf Science*, *55*(6), 857–883. https://doi.org/10.1006/ecss.2002.1033

Twining, B. S., & Baines, S. B. (2013). The Trace Metal Composition of Marine Phytoplankton. *Annual Review of Marine Science*, *5*(1), 191–215. https://doi.org/10.1146/annurev-marine-121211-172322

Unda-Calvo, J., Ruiz-Romera, E., Fdez-Ortiz de Vallejuelo, S., Martínez-Santos, M., & Gredilla, A. (2019). Evaluating the role of particle size on urban environmental geochemistry of metals in surface sediments. *Science of The Total Environment*, *646*, 121–133. https://doi.org/10.1016/j.scitotenv.2018.07.172

Vance, D., Matthews, A., Keech, A., Archer, C., Hudson, G., Pett-Ridge, J., & Chadwick, O. A. (2016). The behaviour of Cu and Zn isotopes during soil development: Controls on the dissolved load of rivers. *Chemical Geology*. https://doi.org/10.1016/j.chemgeo.2016.06.002

Viers, J., Grande, J. A., Zouiten, C., Freydier, R., Masbou, J., Valente, T., Torre, M.-L. de la, Destrigneville, C., & Pokrovsky, O. S. (2018). Are Cu isotopes a useful tool to trace metal sources and processes in acid mine drainage (AMD) context? *Chemosphere*, *193*, 1071–1079. https://doi.org/10.1016/j.chemosphere.2017.11.133

von der Heyden, B. P., & Roychoudhury, A. N. (2015). Application, Chemical Interaction and Fate of Iron Minerals in Polluted Sediment and Soils. *Current Pollution Reports*, *1*(4), 265–279. https://doi.org/10.1007/s40726-015-0020-2

Weber, T., John, S., Tagliabue, A., & DeVries, T. (2018). Biological uptake and reversible scavenging of zinc in the global ocean. *Science*, *361*(6397), 72–76. https://doi.org/10.1126/science.aap8532

Weiss, D. J., Rausch, N., Mason, T. F. D., Coles, B. J., Wilkinson, J. J., Ukonmaanaho, L., Arnold, T., & Nieminen, T. M. (2007). Atmospheric deposition and isotope biogeochemistry of zinc in ombrotrophic peat. *Geochimica et Cosmochimica Acta*, *71*(14), 3498–3517. https://doi.org/10.1016/j.gca.2007.04.026

Wiederhold, J. G. (2015). Metal Stable Isotope Signatures as Tracers in Environmental Geochemistry. *Environmental Science & Technology*, *49*(5), 2606–2624. https://doi.org/10.1021/es504683e

Yang, S.-C., Hawco, N. J., Pinedo-Gonzalez, P., Bian, X., Huang, K.-F., Zhang, R., & John, S. G. (2020). A new purification method for Ni and Cu stable isotopes in seawater provides evidence for widespread Ni isotope fractionation by phytoplankton in the North Pacific. *Chemical Geology*, *547*, 119662. https://doi.org/10.1016/j.chemgeo.2020.119662

Zhang, R., Russell, J., Xiao, X., Zhang, F., Li, T., Liu, Z., Guan, M., Han, Q., Shen, L., & Shu, Y. (2018). Historical records, distributions and sources of mercury and zinc in sediments of East China sea: Implication from stable isotopic compositions. *Chemosphere*, *205*, 698–708. https://doi.org/10.1016/j.chemosphere.2018.04.100

Zhang, Y., Planavsky, N. J., Zhao, M., Isson, T., Asael, D., Wang, C., & Wang, F. (2021). The isotopic composition of sedimentary organic zinc and implications for the global Zn isotope mass balance. *Geochimica et Cosmochimica Acta*, *314*, 16–26. https://doi.org/10.1016/j.gca.2021.09.009

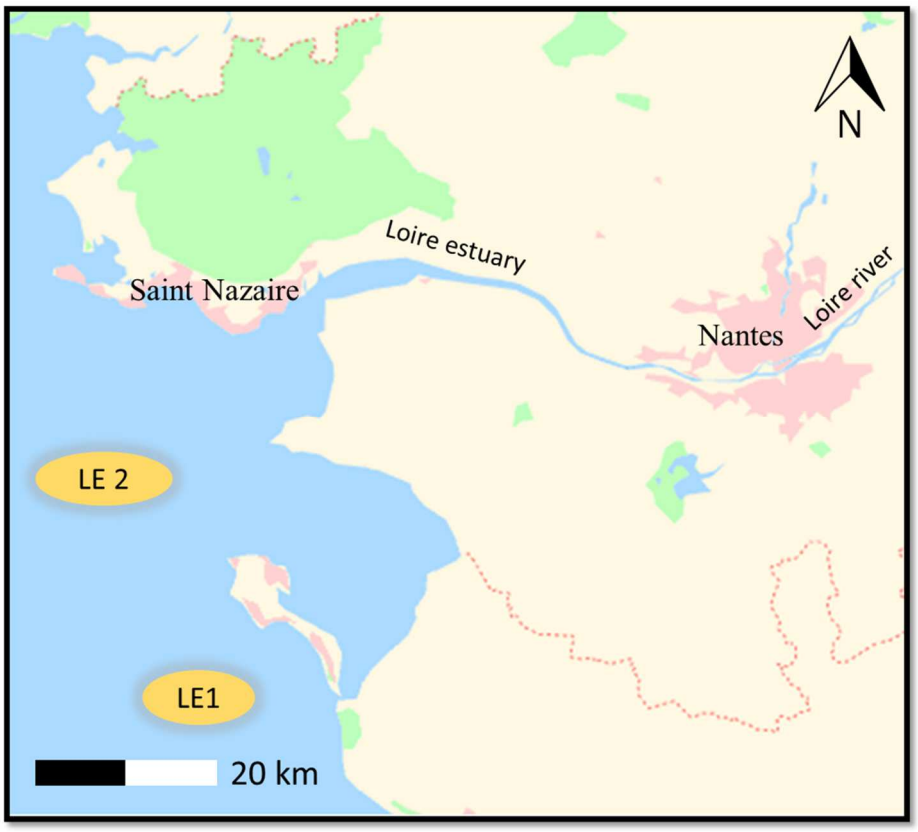

Fig. 1 Sampling stations (LE1 and LE2) for suspended particulate matter in the Northern Bay of Biscay.

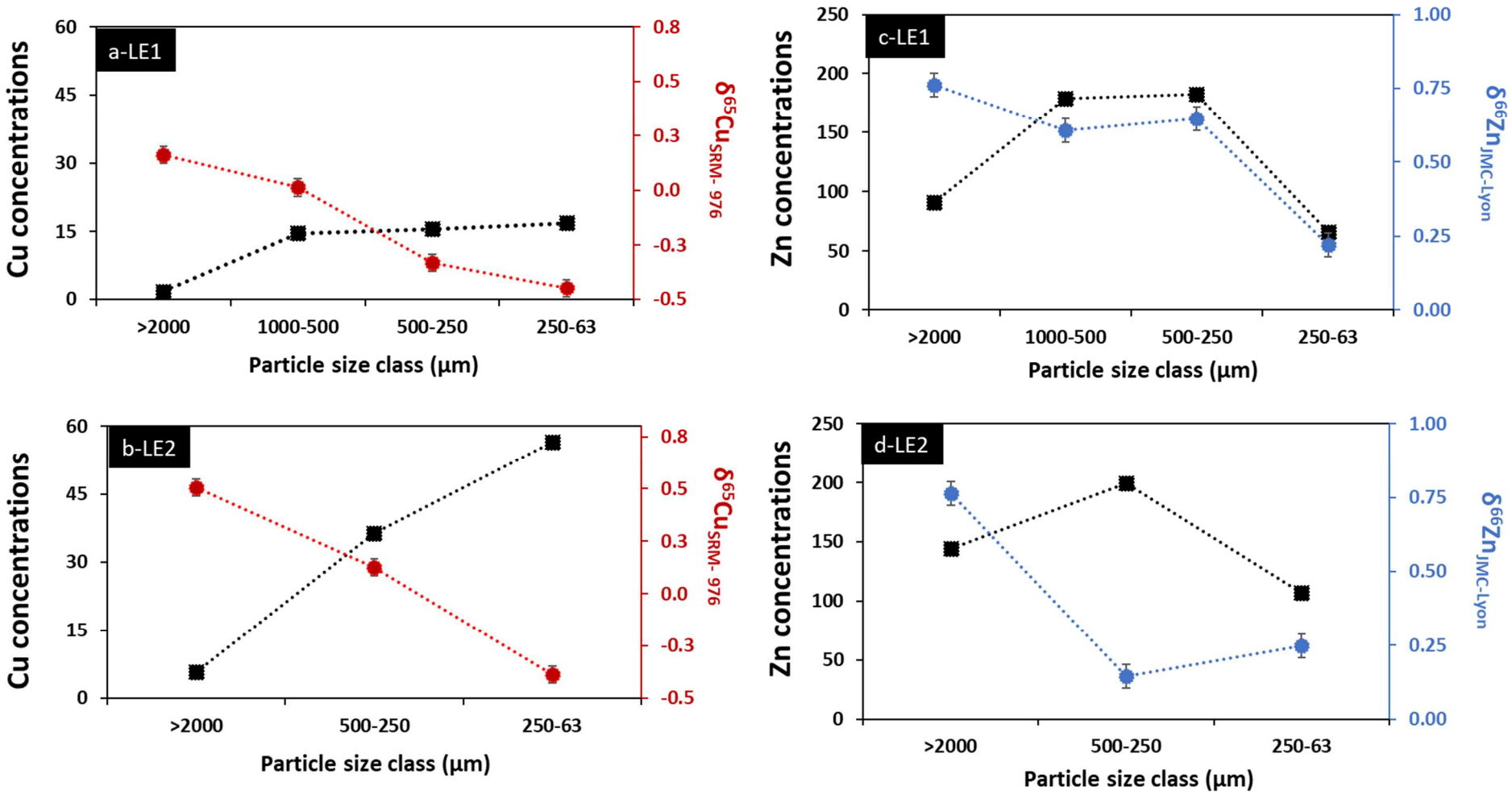

Fig. 2 Concentrations (µg g^{-1}, dry weight) and isotope compositions of Cu and Zn (in per mil, ‰) in SPM sub-fractions collected at the LE1 and LE2 sampling stations. Sub-fractions comprise the different particle size classes of SPM (µm): >2000; 1000-500; 500-250; 250-63. The fraction 1000-5000 µm is missing for LE2 due lack of sufficient material for analyses.

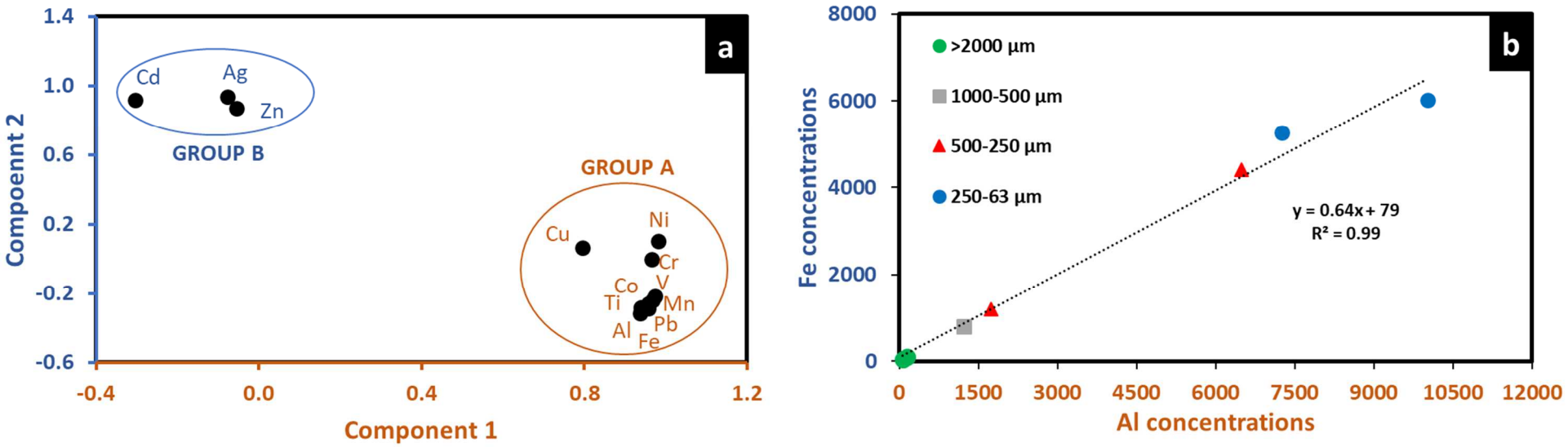

Fig. 3 (a) Principal component analysis for trace and major elemental dataset of SPM and the identification of intercorrelated elements in clusters: Group A and Group B, respectively; **(b)** regression analysis for Fe and Al concentrations (µg g^{-1}, dry weight).

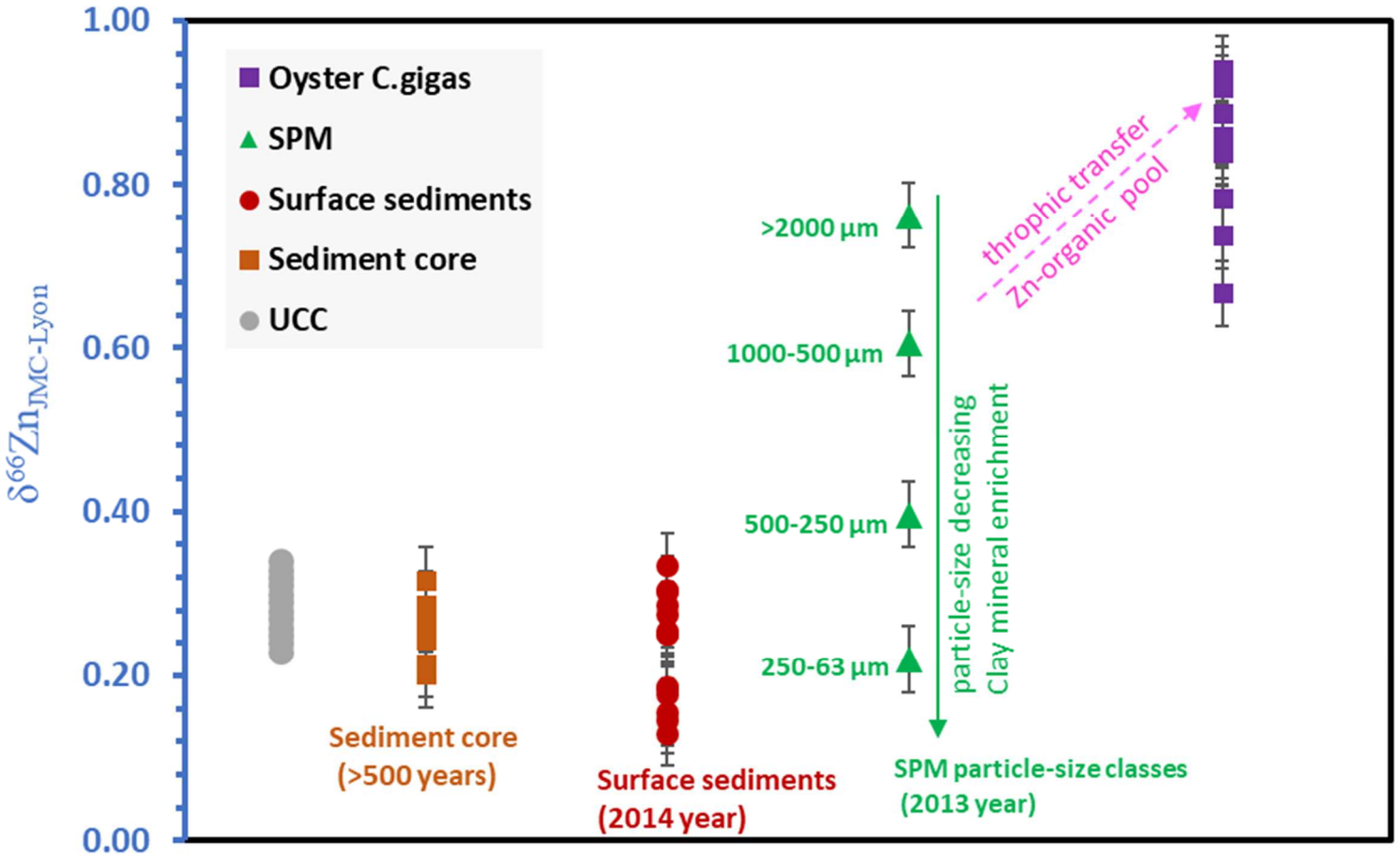

Fig.4 Zn multi-compartmental isotope variability in the Loire estuary and Upper Continental Crust (UCC). δ^{66}Zn value average of SPM particle-size fractions (this study) is compared to sediments (Araújo et al., 2019b) and primary consumers (oysters, Araújo, et al., 2021) reported in previous studies. A sediment core ("PV1") integrate an isotope record of at least 500 years. Zinc isotope range of the UCC is reported by (Moynier et al., 2017). Clay mineral may be coated by Fe and Al oxides and biofilms. As clay minerals contents decrease with particle-size increasing, Zn organic pool becomes prevalent, and the SPM δ^{66}Zn value shifts up. This tendency implies that the Zn-organic pool present in the different SPM fractions presents heavier isotope compositions. Therefore, the high δ^{66}Zn values of oyster's soft tissues are consistent with the hypothesis of bioaccumulation of a local available Zn-organic pool enriched in the heavy Zn isotope.

Table 1. Elemental concentrations (µg g^{-1}, dry weight) and Cu and Zn isotope compositions (‰) dataset for different particle-size fractions of SPM from the Loire estuary mouth. δ-values for Cu and Zn are calculated in relation to the reference materials "NIST-SRM 976" and "JMC-Lyon", respectively. Isotope data for reference materials (RMs) represent the average of replicates, this is, distinct aliquots processed through digestion, chromatography and measured twice or thrice by MC-ICP-MS.

Sample	δ^{65} Cu	2s	δ^{66} Zn	2s	Cu	Zn	Fe	Al	Ti	V	Cr	Mn	Co	Ni	Ag	Cd	Pb
LE1 63-250 µm	-0.45	0.01	0.22	0.01	17	66	6023	10016	233	17.2	13.7	84	1.94	7.0	0.04	0.08	6.9
LE1 250-500 µm	-0.33	0.02	0.65	0.03	16	183	1202	1734	62	3.7	6.1	22	0.52	4.1	0.19	0.48	1.5
LE1 500-1000 µm	0.01	0.06	0.61	0.02	15	179	801	1226	46	2.8	6.7	16	0.38	4.3	0.16	0.45	1.1
LE1 >2000 µm	0.16	0.06	0.76	0.07	2	91	39	63	19	0.2	2.1	1	0.05	1.1	0.04	0.14	0.1
LE2 63-250 µm	-0.39	0.01	0.25	0.00	57	107	5267	7254	162	12.1	15.1	70	1.61	6.8	0.05	0.13	7.5
LE2 250-500 µm	0.12	0.01	0.14	0.02	36	200	4406	6489	161	10.8	18.3	68	1.40	6.5	0.07	0.17	5.5
LE2 >2000 µm	0.51	0.01	0.76	0.04	6	144	93	141	20	0.3	1.0	2	0.05	0.5	0.04	0.21	0.1
Reference Materials																	
BCR 414	-0.27 *n* = 3	0.02	0.23 *n* = 1	0.09													
SRM 1566b	0.23 *n* = 11	0.03	0.70 *n* = 5	0.05													
MESS-3	0.03 *n* = 10	0.08	0.26 *n* = 10	0.06													

Graphic abstract